Published in final edited form as:
Cell Metab. 2008 April ; 7(4): 312–320. doi:10.1016/j.cmet.2008.02.004.

Mice with Mitochondrial Complex I Deficiency Develop a Fatal Encephalomyopathy

Shane E. Kruse[1], **William C. Watt**[1], **David J. Marcinek**[2], **Raj P. Kapur**[3], **Kenneth A. Schenkman**[4], and **Richard D. Palmiter**[1]

1*Howard Hughes Medical Institute and Department of Biochemistry, University of Washington, Seattle, Washington 98195, USA*

2*Department of Radiology, University of Washington, Seattle, Washington 98195, USA*

3*Department of Pathology, Children's Hospital and Regional Medical Center, Seattle, Washington 98195, USA*

4*Department of Pediatrics, University of Washington, Seattle, Washington 98195*

SUMMARY

To study effects of mitochondria complex I (CI, NADH:ubiquinone oxidoreductase) deficiency, we inactivated the *Ndufs4* gene (KO mice), which encodes an 18 kD subunit of the 45-protein complex. Although small, KO mice appeared healthy until ~5 wk of age, when ataxic signs began and progressed until death at ~7 wk. The KO mice manifested encephalomyopathy including a retarded growth rate, lethargy, loss of motor skill, blindness, and elevated serum lactate. CI activity in submitochondrial particles from KO mice was undetectable by spectrophotometric assays. However, CI-driven oxygen consumption by intact tissue was about half that of controls. Native gel electrophoresis revealed reduced levels of intact CI. These data suggest that CI fails to assemble properly or is unstable without Ndufs4. KO muscle has normal morphology but low NADH dehydrogenase activity and subsarcolemmal aggregates of mitochondria. Nonetheless, total oxygen consumption, muscle ATP and phosphocreatine concentrations measured *in vivo* were within normal parameters.

INTRODUCTION

Mitochondria play vital roles in energy production, Ca^{2+} buffering, apoptotic events, and production of reactive oxygen species (ROS) (Nemoto et al., 2000; Sayer, 2002; Schapira, 1996; Smith et al., 2000; Wallace, 1999). Given these essential functions, it is not surprising that mitochondrial failure is implicated in a wide variety of diseases, generally involving tissues with high-energy demand (Coskun et al., 2004; Finsterer, 2006; Kim et al., 2001; Orth and Schapira, 2002; Zeviani et al., 1998). Neural, muscular and cardiac pathologies frequently

Correspondence should be addressed to Richard Palmiter palmiter@u.washington.edu.

AUTHOR CONTRIBUTIONS

S.E.K. completed the spectrophotometric analyses of SMPs, polarography, histological analyses, animal behavior experiments, western and southern analyses, and data analyses as a member of R.D.P.'s laboratory. S.E.K. and R.D.P prepared the manuscript. R.D.P. created the *Ndufs4* targeting construct and performed southern analyses quantifying mitochondrial DNA. W.C.W. carried out BNGE and western analysis. D.J.M. oversaw the *in vivo* NMR and optical spectrometry procedures, and completed related data analyses. Optical spectrometry was performed in the laboratory of K.A.S. R.P.K. performed the electron microscopy.

result from dysfunctional mitochondria and progressive encephalomyopathy is a common clinical phenotype. Mitochondrial CI-associated defects are the most common mitochondrial disorders (Benit et al., 2003; Kirby et al., 1999; Loeffen et al., 2000; Petruzzella and Papa, 2002; Smeitink et al., 2001). CI is the primary entry point for electrons into the electron transport chain (ETC) and is comprised of at least 45 different proteins (Carroll et al., 2006). Defects in the non-enzymatic, nuclear-encoded CI protein, NADH:ubiquinone oxidoreductase iron-sulfur protein 4 (Ndufs4, 18kD) cause a Leigh-like phenotype in humans that results in death within 3–16 months after birth (Budde, 2000, 2003; Petruzzella, 2001; van den Heuvel, 1998). Findings in patients with *NDUFS4* mutations include retarded growth, developmental delay, visual defects, muscular hypotonia, encephalomyopathy, cardiomyopathy, lethargy and failure to thrive (Budde et al., 2003; Petruzzella et al., 2001; Scacco et al., 2003; Ugalde et al., 2004; van den Heuvel et al., 1998). In humans, Ndufs4 appears to be essential for proper assembly of CI (Petruzella et al., 2001, Scacco et al., 2003).

Despite the importance of mitochondria and the many disorders that result from cellular respiratory dysfunction, there are few genetic models of mitochondria-associated disease. Although other mouse models indirectly affect CI activity (Larsson et al., 1998; Park et al., 2007; Vahsen et al., 2004), none consist of a CI-specific mutation. We created a specific mutation of a CI subunit (*Ndufs4*). In this paper, we describe their mitochondrial encephalomyopathy phenotype.

RESULTS

Phenotype of *Ndufs4*-null Mice

Mice with a conditional allele of the *Ndufs4* gene (exon 2 flanked by loxP sites) were generated (Figure S1A, B). Homozygous $Ndufs4^{lox/lox}$ mice appear normal; however, deletion of exon 2 in all cells ($Ndufs4^{\Delta/\Delta}$ =KO) caused the severe phenotype described below. Exon 2 encodes the last part of a mitochondrial targeting sequence and the first 17 amino acids of the mature Ndufs4 protein. Excision of exon 2 produces a frameshift that precludes synthesis of mature Ndufs4 protein. Ndufs4 protein was undetectable in protein extracts from KO mice by Western blot (Figure S1C).

Mice heterozygous (HET) for the deleted *Ndufs4* allele were indistinguishable from wild-type (WT) mice. By postnatal day 21 (P21), most KO mice were smaller than normal and had begun to lose their body hair; however, their hair grew back during the next hair-growth cycle (Figure S2). KO mice reached a maximum body weight of ~15 g at ~P30 (Figure 1A). Prior to P30, the KO mice groomed, fed, responded to novel objects, socialized, and generally behaved similarly to control mice. They had normal locomotor activity during both day and night until ~P30, when they became lethargic (Figure 1B). Total oxygen consumption (Figure 1C), CO_2 clearance, and food consumption by KO mice during both day and night, and during a fast, were within normal ranges when measured over 2 days in metabolic chambers (data not shown), but body temperature was ~2° C lower than controls after P30 (Figure 1D). KO mice were blind, which manifested as an absent B wave in anlectroretinogram (Figure 1E), and by their failure to recognize a visual cliff (data not shown). As early as P20, cataracts sometimes appeared in one or both eyes; after P35, KO mice were often unable to open their eyes completely. The acoustic startle response of KO mice was similar to (and often exceeded) that of controls until ~P35 (Figure 1F). After P35, but with variable time of onset, there was a rapid decline in startle response (Figure 1F, **inset**), such that some older KO mice (n =4) no longer responded tones up to 120 dB. Starting at ~P35, the KO mice developed severe ataxia: they had splayed legs, became unresponsive to a firm nudge, were slow and awkward at righting themselves, and sometimes they would lose their balance and fall over. These older KO mice were unable to maintain balance on a 0.7 mm-wide ledge, they failed a negative geotaxis test, they attempted to clasp a hind leg when suspended by their tail, and they could not remain on

a rotating rod as long as controls (Figure 1G). Light microscopic studies of sections from cerebrum, brainstem, cerebellum, and eye did not reveal any significant differences between KO and WT at P35. In particular, neither infarcts, neuronal loss, nor gliosis were evident in sections stained with either cresyl violet or hematoxylin and eosin (data not shown). Between P35–50 the KO mice stopped gaining weight, their ataxia worsened, they ceased grooming, and died.

Measurement of CI Activity and Abundance

Enriched mitochondrial samples were prepared from liver to measure respiratory capacity. Rotenone–sensitive, CI activity was detected in sub-mitochondrial particles (SMPs) isolated from WT and HET samples, but not from KO samples (Figure 2A). The maximal enzymatic activity of respiratory complex II (CII) of KO mice was significantly higher. Activities of complex III (CIII) and complex IV (CIV) from KO mice were comparable to control samples (Figure 2A), although CIII activity of KO mice tended to be lower.

In contrast to the results obtained with SMPs, CI activity was detectable in intact cells (Figure 2B, C **and** Figure S3). The activities of CI, CII, and CIV were measured by monitoring oxygen consumption using a Clarke electrode. Complex activity measured in this manner implies coupling of a functional respiratory chain with oxygen as the final electron acceptor. Amounts of oxygen consumption by tissue samples from KO and control mice were always measured in parallel. CI activity of tissues from KO mice was about half that of controls, whereas CII and CIV activities were equivalent or slightly higher than controls (Figure 2C). Detection of rotenone-sensitive oxygen consumption in intact tissue, but lack of CI activity in SMPs, suggests that functional CI is unstable during preparation of SMPs in the absence of Ndufs4.

The abundance of CI in mitochondria from liver and brain was assessed by Blue Native Gel Electrophoresis (BNGE). Equal amounts of mitochondria were loaded, electrophoresed, blotted and then probed with antibodies to 3 different CI subunits (Ndufs3, Ndufb6, and Ndufa9) located in different parts of the complex (Figure S4A). The abundance of intact CI was reduced in mitochondria from liver or brain of KO mice compared to controls (Figure 2D). However, SDS-PAGE analysis of the same samples with the three antibodies gave equivalent signals from WT and KO tissue (Figure 2E). These results indicate that although individual subunits of CI are present at comparable amounts, the amount of intact CI is reduced in mitochondria from KO mice, which could account for the lower oxygen consumption by KO tissues.

Muscle Physiology and Metabolite Measurements

We used ^{31}P-NMR spectroscopy to measure ATP turnover reactions and ATP, phosphocreatine (PCr) and inorganic phosphate (P_i) concentrations during hindlimb ischemia reperfusion *in vivo*. Resting O_2 consumption rate was measured using optical spectroscopy of hemoglobin and myoglobin saturations *in vivo*. During ischemia, PCr was depleted, while P_i increased (Figure 3A); when oxygen flow was restored, PCr returned to normal levels. The rate of PCr recovery following ischemia was used to determine the mitochondrial phosphorylation capacity (maximal mitochondrial ATP production). Resting ATP demand (Figure 3B), phosphorylation capacity (Figure 3C), and resting O_2 consumption (data not shown) were not different between the control and KO mice. At the end of the experiment, total muscle ATP and PCr were measured. Muscle from KO mice (age P30) had ATP levels that were at the low end of the normal range, but PCr, Cr and inorganic phosphate (P_i) were normal (Table 1).

Fasting blood glucose concentration of KO mice was not significantly different than controls. KO mice >P40 had slightly elevated serum lactate levels of 1.90 ± 0.19 mM (Table 1), whereas young KO mice (~P18) had lactate levels that were similar to WT mice (data not shown).

Muscle Mitochondria and Histochemistry

The relative number of mitochondrial genomes was quantified by Southern blot analysis of total DNA isolated from brain, heart, kidney, liver, and soleus muscle of control and KO mice (>P35) using a mouse mitochondrial DNA probe. The intensity of the mitochondrial DNA band relative to a nuclear gene from KO tissues was the same as controls (Figure S5).Electron microscopy was used to examine mitochondrial morphology and density in muscle tissue. Mitochondrial ultrastructure appeared normal; although large subsarcolemmal clusters of mitochondria were present in the soleus, but not extensor digitorum longus (EDL) muscle fibers of KO mice (Figure 4A).

Both glycolytic and oxidative muscles of KO mice (>P30) had normal polygonal morphology with peripheral nuclei (Figure 4B). Muscle of control and KO mice appeared normal after staining using the Gomori trichrome method, and there was no evidence of a ragged-red fiber phenotype. All muscle fiber types were present as shown by myofibrillar ATPase staining in various muscles including tibialis anterioris and soleus muscle. Succinate dehydrogenase (SDH) stain intensity often appeared slightly darker for KO mice, although quantitative analysis revealed no difference. There was a marked decrease in NADH oxidase activity in KO muscle fibers, while cytochrome c oxidase (COX) activity was comparable in both control and KO muscle (Figure 4B).

DISCUSSION

We have described the phenotype of a mouse model of CI deficiency caused by mutating one of its 45 subunits. Respiratory CI activity was impaired in the absence of Ndufs4 protein and a fatal phenotype developed, similar to the Leigh-like encephalomyopathy observed in humans with mutations in *NDUFS4*. In the absence of Ndufs4, the abundance of CI and the rate of CI-driven oxygen consumption by intact cells were significantly reduced. Nevertheless, ATP, PCr, glucose, and lactate levels were close to normal and total oxygen consumption by KO mice was unaffected. Although growth retarded, the activity and behavior of KO mice were similar to WT mice during the first 4 wk; this was followed by increasing lethargy, although oxygen consumption remained constant. After P35, the motor abilities of KO mice rapidly deteriorated, they lost weight, and usually died by P50.

We confirmed CI dysfunction in Ndufs4 KO mice. It was surprising that SMPs isolated from mitochondria of KO mice had no detectable CI activity when reduction of an ubiquinone derivative was measured, yet the KO mice lived 5 wk before displaying severe signs of illness, and their total oxygen consumption appeared normal. We suspected that CI was at least partially functional in KO tissue, and confirmed this by monitoring oxygen uptake in intact mitochondria. CI-dependent oxygen consumption (rotenone-sensitive) was evident in tissue from KO mice, although at less than half the rate of control tissue. The residual CI activity in intact mitochondria from KO mice had the same rotenone sensitivity as controls (data not shown). The presence of some intact CI explains why ATP levels of skeletal muscle *in vivo* were normal and that ATP was regenerated after ischemia at a rate equivalent to WT. The activities of the other respiratory complexes were normal, or slightly elevated, in agreement with studies using human fibroblasts and skeletal muscle with *NDUFS4* mutations (Budde et al., 2000; van den Heuvel et al., 1998).

Mutations in human *NDUFS4* also abolish CI activity in SMPs and this loss of activity is associated with appearance of large, sub-complexes, suggesting that the stability or assembly of intact CI is affected (Petruzzella et al., 2001; Scacco et al., 2003). When CI from KO mice was examined by BNGE, the results indicated that the abundance of intact CI was reduced, in agreement with reduced CI activity. There was no evidence of sub-complexes as reported for *NDUFS4* mutations in human fibroblasts. The difference between our results and those

reported for human NDUFS4 mutations could reflect differential effects of the native gel electrophoresis methods used to analyze CI integrity or different stability of the remaining CI components in the absence of Ndufs4 in the two species. Both species exhibit an absence of CI activity in SMPs.

The failure of the spectrophotometric methods to record measurable CI activity may be due to the preparation of SMPs. Sonication, freeze-thaw, or detergents are used to fracture mitochondria and thereby allow access of substrates to the inner mitochondrial membrane. We hypothesize that these manipulations disrupt an already compromised complex resulting in complete loss of activity. The non-functional sub-complex of human Ndufs4-deficient fibroblasts may represent an intermediate of an unstable complex under these conditions. Because humans with complete loss of NDUFS4 survive for several months, we suspect that they too retain some CI activity, and that fibroblast cell lines derived from patients may not represent the situation *in vivo*. Alternatively, mice and humans may respond differently to Ndufs4 deficiency. Our observation that some intact CI can form in the absence of Ndufs4 suggests that this subunit plays an important role in the assembly or stability of the complex, but the intact complex can form without it, perhaps because of compensation by other proteins.

We examined whether metabolite levels were affected by CI deficiency. Serum lactate was slightly higher in the older mice, but not enough to suggest toxic acidosis. The lowered CI activity may result in accumulation of NADH, which would negatively affect energy flux, and reduce lactate dehydrogenase activity. Lactic acidosis occurs in humans with dysfunctional mitochondria, including patients of Leigh syndrome, although not usually in patients with *NDUFS4* mutations, in agreement with our data (Loeffen et al., 2000). Blood glucose levels were also normal. NADH oxidase was reduced in muscle from KO mice, substantiating a CI deficiency. Despite the decrease of NADH oxidase activity, muscle morphology appeared normal, supporting the idea that some functional CI is retained in muscle from KO mice. COX staining of KO mice was comparable, but sometimes appeared slightly less intense than controls in highly oxidative muscle such as the soleus. Lower COX activity has been observed when SDH activity increased (Lopeza et al., 2000; Rifai et al., 2004). The SDH stain in oxidative muscle of KO mice is sometimes more intense than controls, and CII-driven O_2 consumption is often slightly higher than controls. Furthermore, mitochondria isolated from KO mice are capable of supporting significantly higher CII activity, suggesting that CII substrate delivered *in vivo* could have therapeutic properties. Although dysfunctional mitochondria sometimes accumulate to extraordinary quantities in muscle from people with mitochondrial dysfunction (Schmiedel et al., 2003), Southern blot analysis indicated that the mitochondrial genome numbers from muscle and 3 other organs of KO mice were normal. Electron microscopy revealed subsarcolemmal accumulation of mitochondria in a subset of highly oxidative KO muscle fibers. In spite of this, ragged-red muscle fibers, which reflect accumulation of dysfunctional mitochondria in the subsarcolemmal region, were not recognizable by the Gomori trichrome method. This is similar to the histology of muscle taken from human Leigh-syndrome patients and compatible with the observation that total mitochondria content and muscle fiber morphology were normal (Loeffen et al., 2000; Munaro et al., 1997; van den Heuvel et al., 1998).

The KO mice die at an early age, despite levels of ATP and glucose being within normal parameters. The absence of deficits in resting ATP levels and rates of ATP production suggest that compromised basal energetics in peripheral tissue is not the cause of death. However, the inability to produce higher amounts of ATP in tissues that have an increasing need for efficient oxidative phosphorylation, such as in the maturing brain, may cause cumulative detrimental effects. Mice deficient in Ndufs4 only in neurons and glia (Nestin-Cre KO) have a phenotype essentially the same as the complete KO described here (unpublished observations). Indirect effects of CI deficiency could also cause encephalomyopathy. Abnormal mitochondrial

trafficking, altered cell signaling, ROS production, and/or impaired Ca^{2+} buffering may be responsible for the severe phenotype of KO mice. Mn-SOD expression increases when CI deficiency produces oxidative stress (Abid et al., 2004; Robinson et al., 1998); however, Mn-SOD levels in mitochondria from KO mice were normal. Likewise, enhanced levels of superoxides were not detected in human fibroblasts from NDUFS4-deficient patients (Iuso et al., 2006; Piccoli et al., 2006). Furthermore, KO fibroblast and neuron cultures did not have increased ROS or cell death (data not shown), arguing against the role of ROS in CI disease.

The mechanisms of ataxic onset and failure to thrive have not yet been determined, although dysfunctional mitochondria have been associated with a variety of central nervous system disorders and neurodegenerative disease (Coskun et al., 2004; Finsterer, 2006; Kim et al., 2001; Orth and Schapira, 2002; Wallace, 1999; Zeviani et al., 1998). Given that the older KO mice suffer from defective vision, ataxia, loss of acoustic startle response and hypoactivity, it is likely that a neuronal deficiency is responsible for their encephalomyopathy. The exaggerated startle response of KO mice may reflect a loss of inhibitory neuron function (Rajendra, 1994). Furthermore, loss of apoptosis-inducing factor (AIF) results in reduced CI content and affects primarily the brain and retina (Vahsen et al., 2004), emphasizing the sensitivity of neurons to metabolic deficiencies. Interestingly, the KO mice have a lower internal body temperature, which they maintain even when housed at ~4° C for several days or when placed on heating pads at ~42° C (data not shown). This suggests that hypothalamic control of temperature may become defective after P30 (Boulant, 2000; Laurberg et al., 2005) and could be partly responsible for the KO phenotype if protein folding is affected.

The roles of mitochondria and CI in human disease are poorly understood. Progress in this area has been impeded by the lack of suitable animal models for research. The KO mice described here have molecular and behavioral signs resembling human mitochondrial encephalomyopathy, suggesting that the *Ndufs4* KO mouse will be a useful genetic model for studying CI deficiencies. Because we engineered a conditional *Ndufs4* allele, CI deficiency can be restricted to specific cell types and the onset of CI inactivation can be regulated. Thus, by crossing these mice with various Cre-expressor lines, it should be possible to determine in which cells and when CI activity is required for normal physiology, behavior and survival.

EXPERIMENTAL PROCEDURES

Generation of *Ndufs4* KO Mice

To create an animal model for CI deficiency the second exon of *Ndufs4* was flanked by loxP sites using standard gene-targeting techniques in AK18.1 ES cell (129/Sv), the Sv-Neo gene was removed by crossing the mice with Rosa26-FlPer, and then the second exon was deleted by crossing the mice with Mox2-Cre (Figure S1A), which removes exon 2 in germline (Tallquist, M.D. and Soriano, P. (2000). Epiblast-Restricted Cre Expression in MORE Mice: A Tool to Distinguish Embryonic vs. Extra-Embryonic Gene Function, Genesis 26:113–115). Mice heterozygous for the *Ndufs4-null* allele ($Ndufs4^{\Delta/+}$) on a mixed 129/Sv:C57Bl/6 genetic background were interbred to create the homozygous mutant (KO). Absence of Ndufs4 protein was verified by western analyses with antibodies against Ndufs4 (Mitosciences, Eugene OR). KO mice were born from HET crosses at almost the expected Mendelian ratio (WT:HET:KO; 1.4:1.9:1.0, n =790) and could usually be recognized as early as postnatal day 16 (P16) by their sparse fur or small size.

Animal Experiments

All animal experiments were performed with the approval of the Animal Care and Use Committee of the University of Washington. Mice were maintained with rodent diet (5053,

Picolab, Hubbard, OR) and water available *ad libitum* in a vivarium with a 12-hr light-dark cycle at 22° C.

Locomotor Activity

Locomotor activity was measured as laser-beam breaks in locomotor chambers (Columbus Instruments, Columbus, OH). Each experiment lasted 48–72 h, after at least 24 h habituation to the chamber.

Metabolic Activity

WT and KO mice were placed in metabolic cages (Columbus Instruments, Columbus, OH) and measurements of O_2, CO_2, food and water were made for three consecutive days. VO_2 was normalized to lean body mass, which was measured using EcoMRI-100 system (Houston, TX). The ages of mice ranged from P26 to P37. Mice were fed *ad libitum* with ground chow (D5053M, PicoLab), with the exception of the second night when they were food-deprived. The experiment was conducted by The Clinical Nutrition Research Unit - Body Composition and Energy Expenditure Core facility at Harborview Hospital, University of Washington, Seattle, WA.

Body Temperature Monitoring

WT, HET and KO mice were subdermally implanted with temperature-sensitive probes (IPTT300 probe, Bio Medic Data Systems, Seaford, DE) in the scapular region and allowed to recover for at least 7 days prior to monitoring using telemetric receivers. Diurnal body temperature was recorded during two weeks of 12:12 h light:dark cycles at 25° C ambient temperature.

Blood Glucose and Lactate Measurements

Blood was taken from the saphenous vein after an overnight fast. Glucose was measured using B-Glucose HemoCue microcuvettes (Ängelholm, Sweden). Lactate was measured using a lactic acid assay kit (State University of New York, Buffalo NY) after plasma isolation using Becton Dickinson (Franklin Lakes, NJ) serum-separator tubes.

Hearing

Gross hearing ability was assessed by an automated acoustic startle system (San Diego Instruments) that records the amplitude of whole body flinch in response to bursts of white noise (Davis et al., 1982). In a single session, the startle response to bursts of 80, 90, 100, 105, 110, and 120 dB were recorded. Ten rounds of successive sound bursts increasing in amplitude were performed per session.

Ataxia Assays

KO and WT mice were tested for muscular coordination and strength using the ledge test, negative geotaxis test, grip test, and performance on rotarod (San Diego Instuments, San Diego CA) (Supplementary Methods). Hind-limb clasping was observed during a 10-s tail suspension.

Electroretinogram

ERGs were recorded with a gold wire/contact lens electrode on the cornea in collaboration with James Hurley (University of Washington) as previously described[35], [36] (see Supplementary Methods).

Respiratory Complex Assays of Maximal Enzyme Activity

Enriched mitochondrial extracts were made using Dounce homogenization and differential centrifugation to separate mitochondria from other cell membranes and cytosol. Then mitochondria were sonicated for 10 s on ice using a Branson 250 sonifier (Danbury, CT) at 50% pulse and 30% output to generate submitochondrial particles (SMPs) for assay. Respiratory complex activity was determined by recording the change in absorbance of decylubiquinone (DB) or NADH in the presence of specific substrates; inhibitors of specific complexes were added to isolate the contribution of specific complexes (Supplementary Methods).

Polarography

Activities of complexes I, II, and IV were measured by monitoring the rate of oxygen consumption with a oxygen electrode in the presence of the complex-specific substrates and calculated as the fraction that was sensitive to complex-specific inhibitors (Supplementary Methods).

Gel Electrophoreses of Protein or DNA

(See Supplementary Methods).

Nuclear Magnetic Resonance Imaging and Optical Spectroscopy

^{31}P-NMR and optical transmission spectra were performed *in vivo* as described[38, 39] (Supplementary Methods).

Histology and Electron Microscopy

Heamatoxylin & eosin (H&E), ATPase, SDH, COX, Gomori trichrome, and NADH oxidase assays were carried out using snap-frozen tissue dissected from the soleus muscle (Supplementary Methods).

Supplementary Material

Refer to Web version on PubMed Central for supplementary material.

ACKNOWLEDGMENTS

We thank Francisco Perez for suggesting that we make the *Ndufs4* KO mice, Kathy Kafer for injecting targeted ES cells into blastocysts, Nora Meneses for help maintaining the mouse colony, Glenda Froelick and James Hagenzieker for help with histology, Kayoko Ogimoto for metabolic chamber data analyses, the James Hurley laboratory and University of Washington Vision Core Grant for the use of the ERG apparatus, and the Conley, Kushmerick, and Schenkman laboratories (in particular Wayne Ciesielski and Lori Arakaki) for the NMR and optical spectra analyses. This work was supported in part by NIH grants AG-022385, AG-028455, and 5P30EY001730.

REFERENCES

Abid MR, Schoots IG, Spokes KC, Wu SQ, Mawhinney C, Aird WC. Vascular endothelial growth factor-mediated induction of manganese superoxide dismutase occurs through redox-dependent regulation of forkhead and IkappaB/NF-kappaB. J. Biol. Chem 2004;279:44030–44038. [PubMed: 15308628]

Benit P, Steffann J, Lebon S, Chretien D, Kadhom N, de Lonlay P, Goldenberg A, Dumez Y, Dommergues M, Rustin P, et al. Genotyping microsatellite DNA markers at putative disease loci in inbred/multiplex families with respiratory chain complex I deficiency allows rapid identification of a novel nonsense mutation (IVS1nt -1) in the NDUFS4 gene in Leigh syndrome. Hum. Genet 2003;112:563–566. [PubMed: 12616398]

Blei ML, Conley KE, Kushmerick MJ. Separate measures of ATP utilization and recovery in human skeletal muscle. J. Physiol 1993;465:203–222. [PubMed: 8024651]

Boulant JA. Role of the preoptic-anterior hypothalamus in thermoregulation and fever. Clin. Infect. Dis 2000;31:S157–S161. [PubMed: 11113018]

Budde SM, van den Heuvel LP, Janssen AJ, Smeets RJ, Buskens CA, DeMeirleir L, Van Coster R, Baethmann M, Voit T, Trijbels JM, Smeitink JA. Combined enzymatic complex I and III deficiency associated with mutations in the nuclear encoded NDUFS4 gene. Biochem. Biophys. Res. Commun 2000;18:63–68. [PubMed: 10944442]

Budde SMS, van den Heuvel LP, Smeets RJ, Skladal D, Mayr JA, Boelen C, Petruzzella V, Papa S, Smeitink JA. Clinical heterogeneity in patients with mutations in the NDUFS4 gene of mitochondrial complex I. J. Inherit. Metab. Dis 2003;26:813–815. [PubMed: 14765537]

Carroll J, Fearnley IM, Skehel JM, Shannon RJ, Hirst J, Walker JE. Bovine complex I is a complex of 45 different subunits. J. Biol. Chem 2006;281:32724–32727. [PubMed: 16950771]

Coskun PE, Beal MF, Wallace DC. Alzheimer's brains harbor somatic mtDNA control-region mutations that suppress mitochondrial transcription and replication. Proc. Natl. Acad. Sci. USA 2004;101:10726–10731. [PubMed: 15247418]

Davis M, Gendelman DS, Tischler MD, Gendelman PM. A primary acoustic startle circuit: lesion and stimulation studies. J. Neurosci 1982;6:791–805. [PubMed: 7086484]

Finsterer J. Central nervous system manifestations of mitochondrial disorders. Acta. Neurol. Scand 2006;114:217–238. [PubMed: 16942541]

Iuso A, Scacco S, Piccoli C, Bellomo F, Petruzzella V, Trentadue R, Minuto M, Ripoli M, Capitanio N, Zeviani M, Papa S. Dysfunctions of cellular oxidative metabolism in patients with mutations in the NDUFS1 and NDUFS4 genes of complex I. J. Biol. Chem 2006;281:10374–10380. [PubMed: 16478720]

Kim SH, Vlkolinsky R, Cairns N, Fountoulakis M, Lubec G. The reduction of NADH ubiquinone oxidoreductase 24- and 75-kDa subunits in brains of patients with Down syndrome and Alzheimer's disease. Life Sci 2001;68:2741–2750. [PubMed: 11400916]

Kirby DM, Crawford M, Cleary MA, Dahl HH, Dennett X, Thorburn DR. Respiratory chain complex I deficiency: an under diagnosed energy generation disorder. Neurology 1999;52:1255–1264. [PubMed: 10214753]

Larsson NG, Wang J, Wilhelmsson H, Oldfors A, Rustin P, Lewandoski M, Barsh GS, Clayton DA. Mitochondrial transcription factor A is necessary for mtDNA maintenance and embryogenesis in mice. Nat Genet 1998;18:199–200. [PubMed: 9500531]

Laurberg P, Andersen S, Karmisholt J. Cold adaptation and thyroid hormone metabolism. Horm. Metab. Res 2005;37:545–549. [PubMed: 16175491]

Loeffen JL, Smeitink JA, Trijbels JM, Janssen AJ, Triepels RH, Sengers RC, van den Heuvel LP. Isolated complex I deficiency in children: clinical, biochemical and genetic aspects. Hum. Mutat 2000;15:123–134. [PubMed: 10649489]

Lopeza ME, Van Zeelanda NL, Dahlb DB, Weindruchc R, Aiken JM. Cellular phenotypes of age-associated skeletal muscle mitochondrial abnormalities in rhesus monkeys. Mut. Res. Fund. Mol. Mech. Mut 2000;452:123–138.

Lyubarsky AL, Lem J, Chen J, Falsini B, Iannaccone A, Pugh EN Jr. Functionally rodless mice: transgenic models for the investigation of cone function in retinal disease and therapy. Vision Res 2002;42:401–415. [PubMed: 11853756]

Marcinek DJ, Schenkman KA, Ciesielski WA, Lee D, Conley KE. Reduced mitochondrial coupling in vivo alters cellular energetics in aged mouse skeletal muscle. J. Physiol 2005;569:467–473. [PubMed: 16254011]

Munaro M, Tiranti V, Sandona D, Lamantea E, Uziel G, Bisson R, Zeviani M. Single cell complementation class is common to several cases of cytochrome c oxidase-defective Leigh's syndrome. Hum. Molec. Genet 1997;6:221–228. [PubMed: 9063742]

Nemoto S, Takeda K, Yu ZX, Ferrans VJ, Finkel T. Role for mitochondrial oxidants as regulators of cellular metabolism. Mol. Cell. Biol 2000;20:7311–7318. [PubMed: 10982848]

Orth M, Schapira AH. Mitochondrial involvement in Parkinson’s disease. Neurochem. Int 2002;40:533–541. [PubMed: 11850110]

Park C, Asin-Cayuela J, Cámara Y, Shi Y, Pellegrini M, Gaspari M, Wibom R, Hultenby K, Erdjument-Bromage H, Tempst P, et al. MTERF3 Is a Negative Regulator of Mammalian mtDNA Transcription. Cell 2007;130:273–285. [PubMed: 17662942]

Petruzzella V, Papa S. Mutations in human nuclear genes encoding for subunits of mitochondrial respiratory complex I: the NDUFS4 gene. Gene 2002;286:149–154. [PubMed: 11943471]

Petruzzella V, Vergari R, Puzziferri I, Boffoli D, Lamantea E, Zeviani M, Papa S. A nonsense mutation in the NDUFS4 gene encoding the 18 kDa (AQDQ) subunit of complex I abolishes assembly and activity of the complex in a patient with Leigh-like syndrome. Hum. Mol. Genet 2001;10:529–535. [PubMed: 11181577]

Piccoli C, Scacco S, Bellomo F, Signorile A, Iuso A, Boffoli D, Scrima R, Capitanio N, Papa S. cAMP controls oxygen metabolism in mammalian cells. FEBS Letters 2006;580:4539–4543. [PubMed: 16870178]

Rajendra S, Lynch JW, Pierce KD, French CR, Barry PH, Schofield PR. Startle disease mutations reduce the agonist sensitivity of the human inhibitory glycine receptor. J. Biol. Chem 1994;269:18739–18742. [PubMed: 7518444]

Rifai Z, Welle S, Kamp C, Thornton CA. Ragged red fibers in normal aging and inflammatory myopathy. Annal. Neurol 2004;37:24–29. [PubMed: 7818253]

Robinson BH. Human complex I deficiency: clinical spectrum and involvement of oxygen free radicals in the pathogenicity of the defect. Biochem. Biophys. Acta 1998;1364:271–286. [PubMed: 9593934]

Saari JC, Nawrot M, Kennedy BN, Garwin GG, Hurley JB, Huang J, Possin DE, Crabb JW. Visual cycle impairment in cellular retinaldehyde binding protein (CRALBP) knockout mice results in delayed dark adaptation. Neuron 2001;29:739–748. [PubMed: 11301032]

Sayer RJ. Intracellular Ca2+ handling. Adv. Exp. Med. Biol 2002;513:183–196. [PubMed: 12575821]

Scacco S, Petruzzella V, Budde S, Vergari R, Tamborra R, Panelli D, van den Heuvel LP, Smeitink JA, Papa S. Pathological mutations of the human NDUFS4 gene of the 18-kDa (AQDQ) subunit of complex I affect the expression of the protein and the assembly and function of the complex. J. Biol. Chem 2003;278:44161–44167. [PubMed: 12944388]

Schapira AH. Oxidative stress and mitochondrial dysfunction in neurodegeneration. Curr. Opin. Neurol 1996;9:260–264. [PubMed: 8858182]

Schmiedel J, Jackson S, Schäfer J, Reichmann H. Mitochondrial cytopathies. J. Neurol 2003;250:267–277. [PubMed: 12638015]

Smeitink J, Sengers R, Trijbels F, van den Heuvel L. Human NADH:ubiquinone oxidoreductase. J. Bioenerg. Biomembr 2001;33:259–266. [PubMed: 11695836]

Smith MA, Rottkamp CA, Nunomura A, Raina AK, Perry G. Oxidative stress in Alzheimer's disease. Biochim. Biophys. Acta 2000;1502:139–144. [PubMed: 10899439]

Tallquist MD, Soriano P. Epiblast-Restricted Cre Expression in MORE Mice: A Tool to Distinguish Embryonic vs. Extra-Embryonic Gene Function. Genesis 2000;26:113–115. [PubMed: 10686601]

Ugalde C, Janssen RJ, van den Heuvel LP, Smeitink JA, Nijtmans LG. Differences in assembly or stability of complex I and other mitochondrial OXPHOS complexes in inherited complex I deficiency. Hum. Mol. Genet 2004;15:659–667. [PubMed: 14749350]

Vahsen N, Cande C, Briere JJ, Benit P, Joza N, Larochette N, Mastroberardino PG, Pequignot MO, Casares N, Lazar V, et al. AIF deficiency compromises oxidative phosphorylation. EMBO J 2004;23:4679–4689. [PubMed: 15526035]

van den Heuvel L, Ruitenbeek W, Smeets R, Gelman-Kohan Z, Elpeleg O, Loeffen J, Trijbels F, Mariman E, de Bruijn D, Smeitink J. Demonstration of a new pathogenic mutation in human complex I deficiency: a 5-p duplication in the nuclear gene encoding the 18-kD (AQDQ) subunit. Am. J. Hum. Genet 1998;62:262–268. [PubMed: 9463323]

Vogel RO, van den Brand MA, Rodenburg RJ, van den Heuvel LP, Tsuneoka M, Smeitink JA, Nijtmans LG. Investigation of the complex I assembly chaperones B17.2L and NDUFAF1 in a cohort of CI deficient patients. Mol. Genet. Metab 2007;91:176–182. [PubMed: 17383918]

Wallace DC. Mitochondrial diseases in man and mouse. Science 1999;283:1482–1488. [PubMed: 10066162]

Zeviani M, Tiranti V, Piantadosi C. Mitochondrial disorders. Molec. Med 1998;77:59–72.

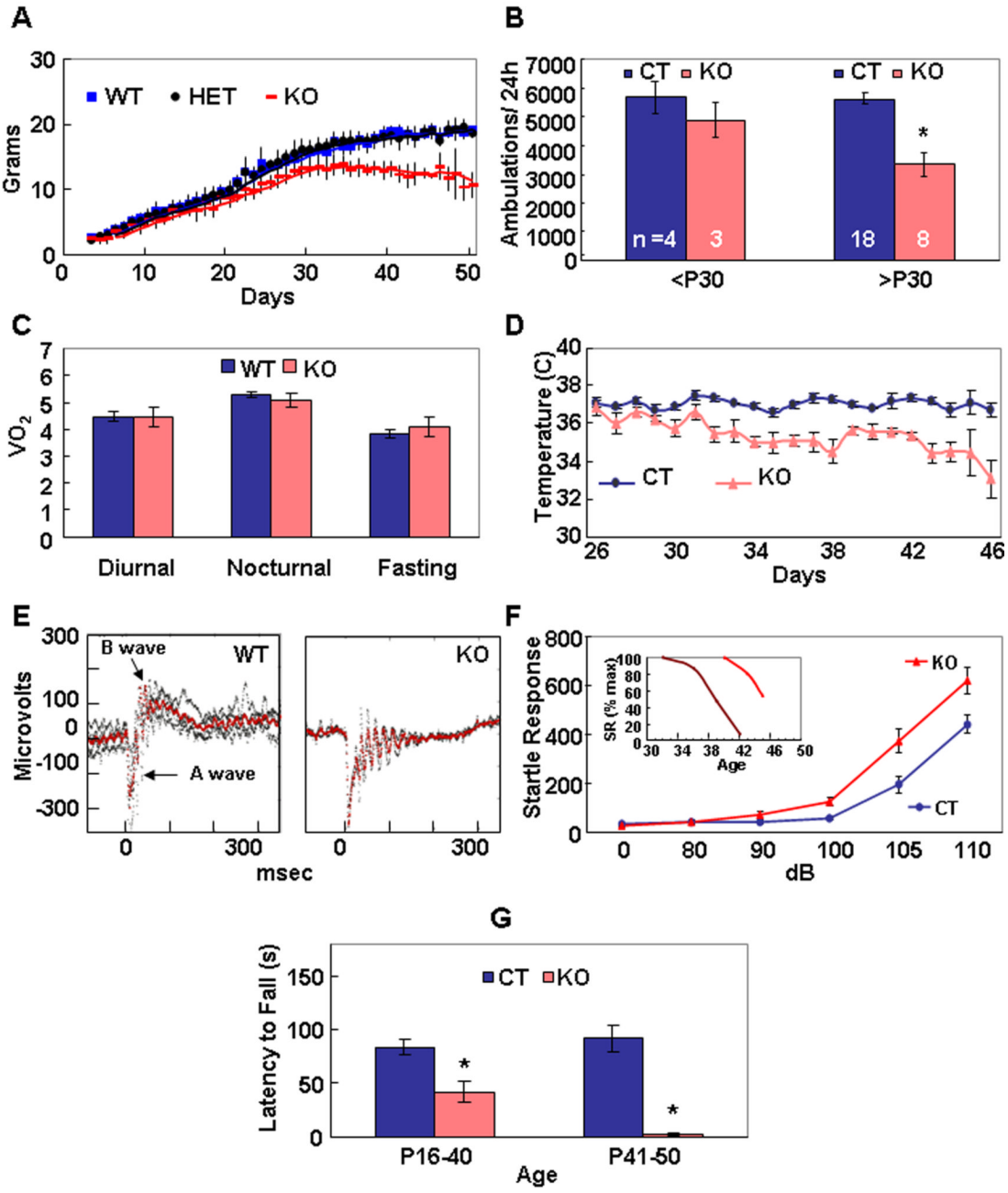

Figure 1. Phenotypes of *Ndufs4* KO Mice

(A) Growth curves of WT, HET and KO female mice. KO mice weigh significantly less than either HET or WT. n =4 to 56, depending on day and genotype. Values given as mean ± s.d. $p < 0.05$ for all time points beyond P15, Student's two-tailed t-test.

(B) Locomotor activity of young (<P30) KO mice is comparable to WT and HET (CT), but older (>P30) KO mice become hypoactive. *, a significant difference ($p = 0.0001$, Student's two-tailed t-test) was obtained between old CT mice and old KO mice. Values given as mean ± s.e.m.

(C) Oxygen consumption (liter/kg lean mass/hr) by KO mice (P26 to P37) during 72 hr in metabolic chambers was the same as controls during daytime, nighttime and fasting. n =9 (WT),

7 (KO), p =0.5 and greater for diurnal, fasting and nocturnal measurements. Values given as mean ± s.e.m.

(D) Body temperature of KO mice older than P30 was ~2°C lower than controls. n =3–9, depending on day and genotype. p <0.001 for all days beyond P30, Student's two-tailed t-test. Values given as mean ± s.e.m.

(E) Electroretinograms indicate that KO mice (P21) lack the B-wave, indicating failure of neurotransmission from photoreceptors to bipolar cells. Superimposed traces from 4 WT and 2 KO mice.

(F) Startle responses (arbitrary units) of KO mice were enhanced relative to WT mice until P36. n =14 (WT <P36), 14 (KO <P36). Values given as mean ± s.e.m. *, p <0.0001 for 90, 100, 105, and 110 dB. Student's two-tailed t-test. *Inset*, Repeated measurements of older KO mice (2 examples shown) reveal progressive loss of startle response, but with variable age of onset; SR (% max) is the percent of maximum startle response.

(G) Rotarod performance (latency to fall) of young (<P20) KO mice is normal; however, at older ages their performance is significantly worse than WT mice. By P40, KO mice could not remain on an immobile Rotarod long enough to begin the experiment. n >20 (CT), n =4 (KO). Values given as mean ± s.e.m. *, p <0.0003 for all ages beyond P21, Student's two-tailed t-test.

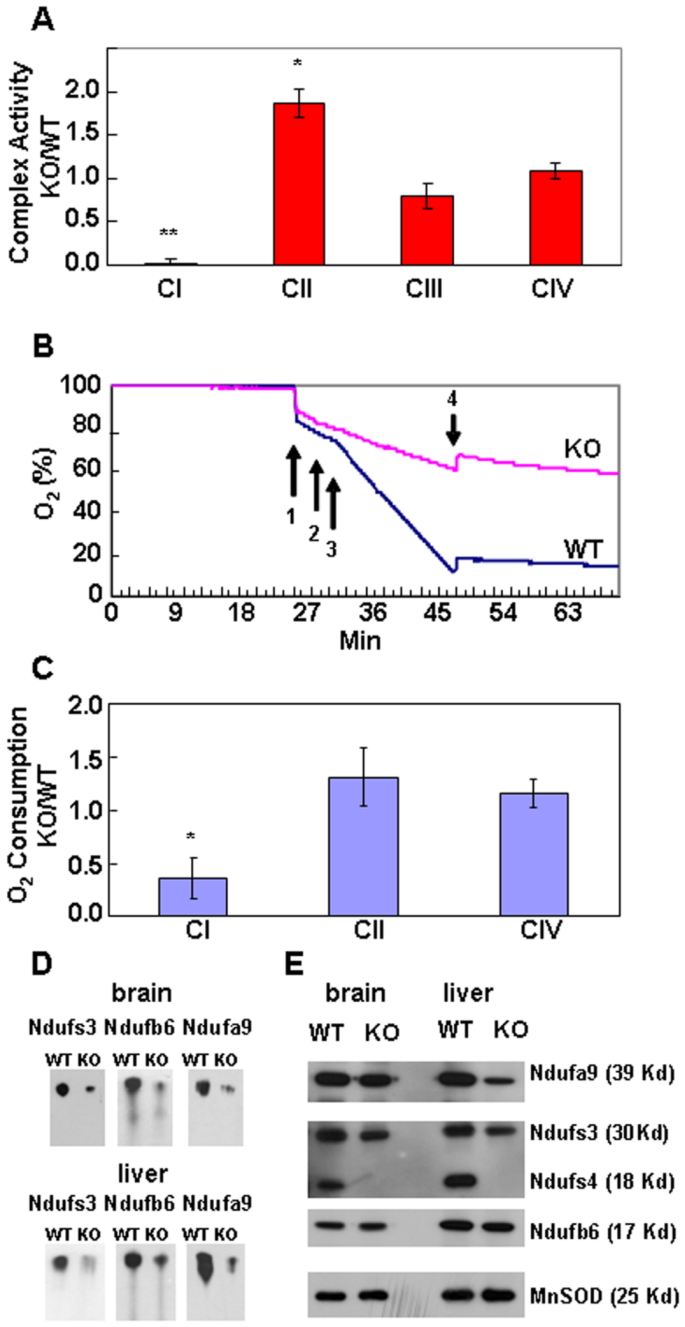

Figure 2. Respiratory Activities

(A) SMPs derived from KO liver had no CI activity, whereas CIII and CIV activities were not significantly different. CII activity was significantly higher. Data were normalized to citrate synthase activity (Δ Abs/min of respiratory complex activity : Δ Abs/min citrate synthase activity); hence they have no units. Assays in triplicate, n =12 for CI, CII, CIV; n =4 CIII. *, p =0.003; **, p =0.0001, Mann-Whitney test. Similar results were obtained with SMPs from brain and MEFs. Values given as mean ± s.e.m.

(B) Rates of O_2 consumption by liver CI from WT and KO mice (P35) were measured. Arrows indicate addition of: (1) tissue, (2) ADP, (3) malate/pyruvate, and (4) rotenone. There was less

O_2 consumption by KO tissue in the presence of malate/pyruvate (CI) relative to WT, and it stopped with addition of rotenone.

(C) The ratio O_2 consumption (oxygen/mg tissue/min) by liver from KO versus WT mice. Complex I activity of KO tissue is less than half that of WT, whereas CII and CIV activities do not significantly differ, n =5. Values given as mean ± s.e.m. *, p =0.0001, Student's two-tailed t-test. Similar results were obtained from brain and muscle.

(D) Blue Native Gel Electrophoresis (BNGE) of CI from brain and liver mitochondria. Proteins representing the three major CI subcomplexes were examined by Western blot; in each case, KO mitochondria had less intact complex I.

(E) SDS PAGE of proteins representing the three major subcomplexes of respiratory complex I. Equivalent amounts of mitochondrial protein were loaded, MnSOD was used as internal standard. The samples were the same as used for the BNGE experiment (Fig. 2D).

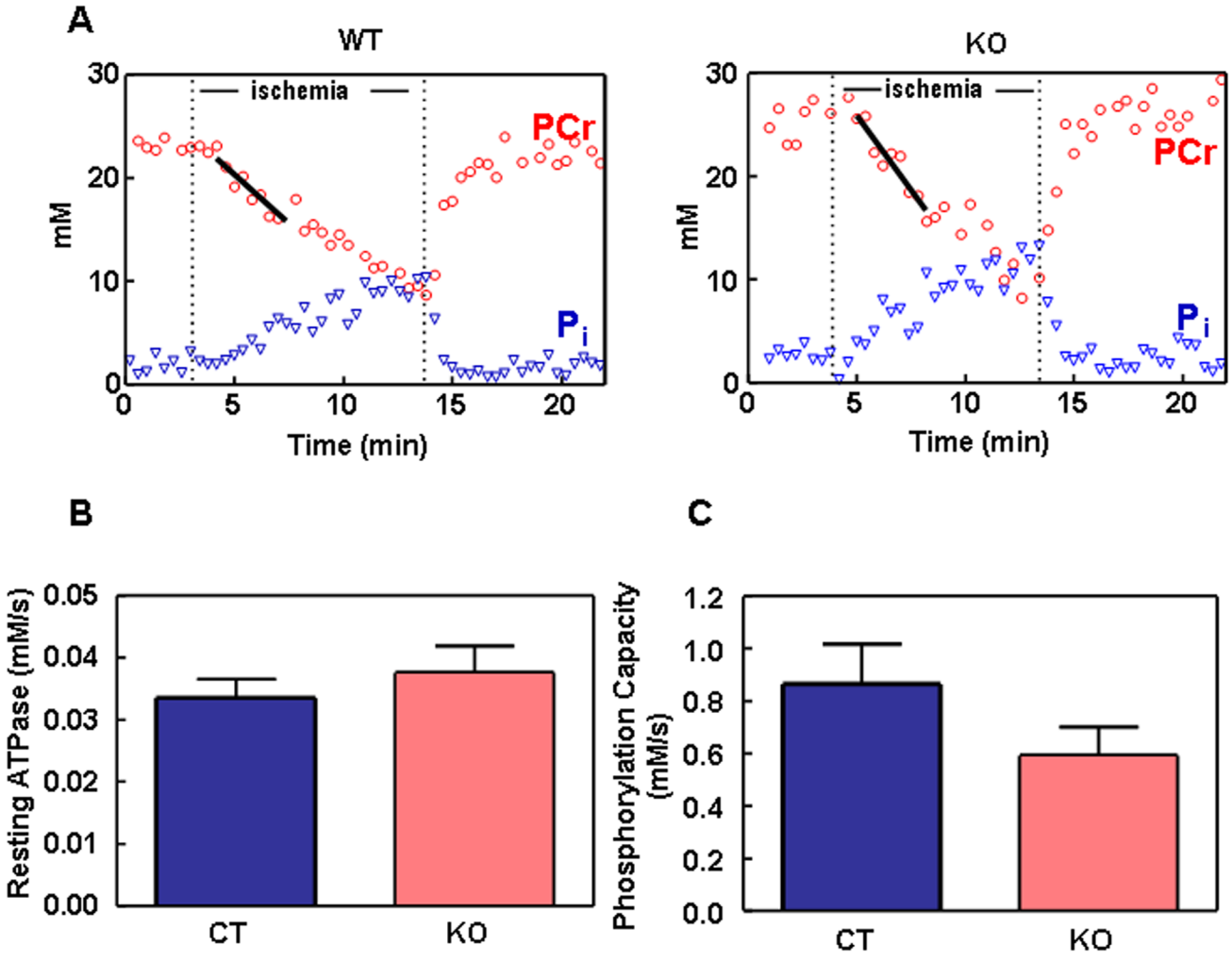

Figure 3. ATP Turnover Reactions During Ischemia Reperfusion in Hindlimb Muscles *in vivo*

(A) Representative data illustrating PCr and P_i dynamics during ischemia and reperfusion. Resting ATPase (equivalent to ATP demand) is equal to the initial rate of PCr breakdown during ischemia (black regression line). The phosphorylation capacity is calculated from the recovery of PCr following ischemia (Bliel et al., 1993).

(B) Resting mitochondrial ATP production (equal to resting ATP demand) is not different in WT (black bars) and KO (open bars) mice. Values given as mean ± s.e.m. (c) The phosphorylation capacity is not significantly different in the skeletal muscle of the WT and KO mice, P =0.12; n =6 for both WT and KO groups. Values given as mean ± s.e.m.

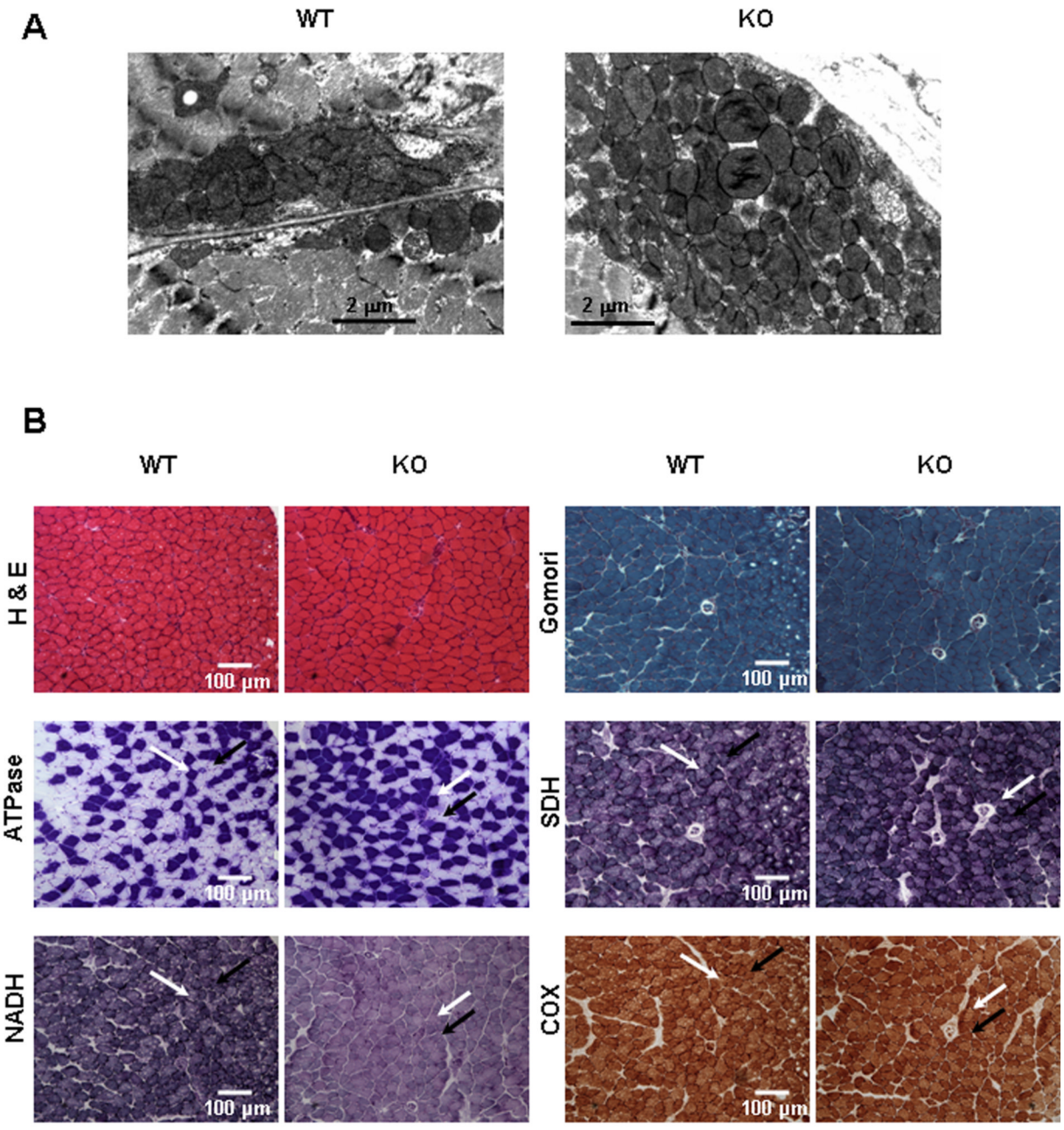

Figure 4. Histological Comparisons of Muscle from KO and WT Mice

(A) Electron microscopic images of the subsarcolemmal layer of soleus muscle (P35). Larger subsarcolemmal clusters of mitochondria (6 or more mitochondria deep) were observed in 50% of soleus muscle fibers from KO mice versus no fibers with clusters greater than 5 mitochondria deep in WT soleus.

(B) Light microscopy of muscle from a WT and KO mouse (age P23, soleus; a highly oxidative muscle). Glycolytic (yellow arrows) and oxidative fibers (red arrows) are indicated. **H & E,** Haemotoxylin and eosin staining. **Gomori** trichrome staining; there are no "ragged-red" fibers. Myofibrillar **ATPase** staining reveals fiber types. Quantitative analysis of slides of 4 mice of each genotype revealed no significant difference in fraction of glycolytic fibers. **SDH** assay

stain intensity often appears slightly darker for KO mice, especially in oxidative muscle fibers identified by ATPase staining. Quantitative analysis of slides of 5 mice of each genotype revealed no significant difference. **NADH** oxidase activity of soleus muscle is lower in KO muscle fibers, primarily in the slow oxidative type (type I, black arrows); white arrows point to glycolytic (type IIB) fibers. **COX**, Cytochrome oxidase staining of KO mice is comparable to WT.

Table 1

Concentrations of Metabolites in Muscle (μmol/gram wet weight for ATP, P_i, PCr and free Cr), and Blood (mM for glucose and lactate, ± s.e.m.)

Genotype	ATP	Inorganic phosphate	Phospho-creatine	Creatine	Glucose	Lactate
WT	9.13±0.50	4.04±0.68	26.89±1.98	13.31±2.01	7.98±0.49	1.4±0.09
KO	7.85±0.59	3.09±0.40	25.77±2.28	15.08±1.42	7.48±1.32	1.9±0.19*

P30 mice were used to measure ATP, P_i, PCr and Cr by high-pressure, liquid chromatography using a photodiode array detector; n=6 (WT) and n=5 (KO). For lactate assay: P18–56 (WT and HET (CT)) n =14, P >40 n =6, (KO).

* p =0.001, Student's two-tailed t-test. For glucose assay: n =22 (CT) n =13 (KO), p =0.12, Student's two-tailed t-test.